



Contents lists available at ScienceDirect

# Bioorganic & Medicinal Chemistry Letters

journal homepage: [www.elsevier.com/locate/bmcl](http://www.elsevier.com/locate/bmcl)

## Studies of cannabinoid-1 receptor antagonists for the treatment of obesity: Hologram QSAR model for biarylpyrazolyl oxadiazole ligands

Mao Ye\*, Marcia I. Dawson

Burnham Institute for Medical Research, La Jolla, CA 92037, USA

### ARTICLE INFO

#### Article history:

Received 19 December 2008

Revised 15 April 2009

Accepted 17 April 2009

Available online 22 April 2009

#### Keywords:

HQ SAR

CB<sub>1</sub>

Antagonist

Fragments

### ABSTRACT

Hologram QSAR studies were conducted on a series of 60 training set of cannabinoid-1 receptor (CB<sub>1</sub>) antagonists. Significant cross-validated correlation coefficients ( $q^2 = 0.763$ ) and noncross-validated correlation coefficients ( $r^2 = 0.897$ ) were obtained. The model was then employed to predict the biological activities of 15 test set compounds, and a good agreement between the experimental and predicted values was verified exhibiting a powerful predictable capability of this model ( $q^2_{\text{pred}} = 0.868$ ). Contribution map shows that 1,2,4-triazole and cyclopropane moieties make big contributions for the activities. Both the HQ SAR model and analysis from the contribution map should be useful for the further design of novel structurally related CB<sub>1</sub> antagonists.

Published by Elsevier Ltd.

The endocannabinoid system (ECS) affects metabolic pathways through expression in the brain and peripheral tissues.<sup>1,2</sup> It has been reported that stimulation of ECS increases the food intake and promotes weight gain, whereas pharmacologic blockade of the system might cause the loss of appetite, representing an effective approach for the therapy of obesity and other metabolic disorders.<sup>3</sup> The ECS comprises of cannabinoid receptors, endogenous ligands and the enzymes which catalyze the synthesis and degradation of endocannabinoids.<sup>4,5</sup> The two cannabinoid receptor subtypes, CB<sub>1</sub> and CB<sub>2</sub>, with increasing reports suggesting the existence of a new type CB<sub>3</sub>,<sup>6–8</sup> belong to the G-protein-coupled receptor (GPCR) superfamily.<sup>9</sup> CB<sub>1</sub> receptor, first identified in 1988<sup>10</sup> and cloned in 1990, was found abundantly in brain neurons.<sup>11</sup> CB<sub>1</sub> receptor antagonist has recently received great attention because it both leads to weight loss and reverses the metabolic effects of obesity, such as hyperlipidemia and insulin resistance.<sup>12</sup> The first clinically used anti-obesity drug based on CB<sub>1</sub> receptor antagonist is rimonabant (SR141716, Fig. 1),<sup>13</sup> approved by European Medical Agency (EMA) in 2006. Other two CB<sub>1</sub> receptor antagonists (otenabant, CP-945598 and MK-0364, taranabant, Fig. 1) have also been accessed to different phase of clinical trials.<sup>14</sup> Up to now, most of the CB<sub>1</sub> antagonists in clinical trials are bioisosteres or conformationally constrained analogues of rimonabant.<sup>15</sup> Recently, Lee et al. reported<sup>16</sup> that the amide group in rimonabant structure can be replaced with imine-type moiety, such as 1,3,4-oxadiazole, imidazoles, and tetrazoles. Among these bioisosteres, the 1,3,4-oxadiazole heterocycle is of particular inter-

est for its introduction of a favorable balance of potency and physicochemical properties which are amenable for further in vivo efficacy evaluation. Through lead optimization, they identified compound **58** to be a better CB<sub>1</sub> inhibitor and a promising candidate for further evaluation as an anti-obesity agent.

Hologram quantitative structure–activity relationships (HQ SAR) are a 2D-QSAR program without need of 3D structure determination, conformation search and molecular alignment.<sup>17</sup> In HQ SAR, each molecule in the training set is divided into several structural fragments, which are arranged to form a molecular hologram, assigned by a cyclic redundancy check (CRC) algorithm. All possible molecular fragments (linear, branched and overlapping) and the numbers of occurrences are counted to generate HQ SAR descriptors. With HQ SAR technique, we can easily and rapidly generate QSAR models for both small and large data set with high predictive value comparable with other 3D QSAR techniques, such as CoMFA and CoMSIA, but much simpler to use.<sup>18</sup> In addition, HQ SAR models interpret positive and negative contributions based on various atoms and structural units, which are alternatives to 3D QSAR models. The limitation of HQ SAR models is that it could not make biological activity predictions accurately to molecules lacking fragments or structural units included in the training data set which are used to set up the model. Although several papers have been published for the 3D-QSAR studies of CB<sub>1</sub> receptor antagonists, HQ SAR studies of these receptor antagonists have rarely been reported.<sup>19</sup> In the present study, we tried to generate and evaluate a HQ SAR model using a total of 75 biarylpyrazolyl oxadiazole ligands as a training set and test set. We hope that these models and analysis will be helpful for the future rational design of novel structurally related CB<sub>1</sub> receptor antagonists.<sup>20</sup>

\* Corresponding author. Tel.: +1 858 6463100/3712; fax: +1 858 6463197.

E-mail address: [maoye@burnham.org](mailto:maoye@burnham.org) (M. Ye).

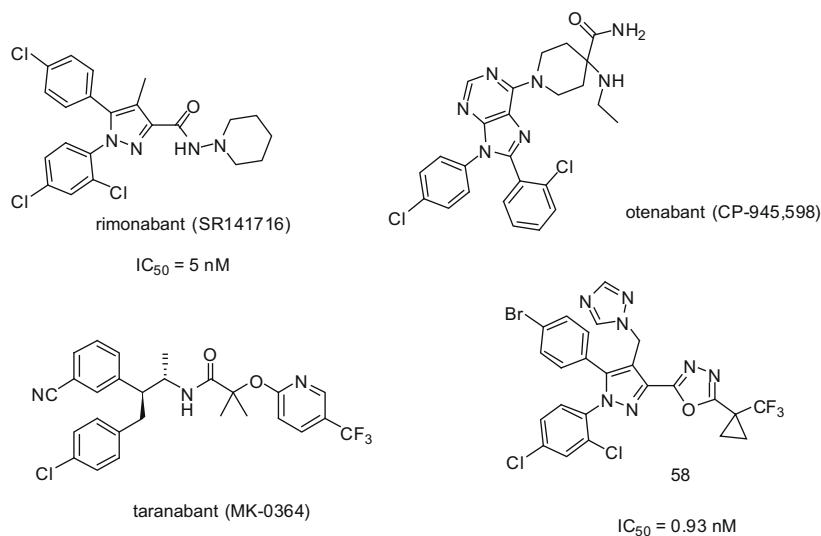


**Figure 1.** Structures of rimonabant, otenabant, taranabant and compound **58**.

A series of biarylpyrazolyl oxadiazole antagonists were taken from the recent publication.<sup>16</sup> Out of 77 reported compounds, two of them were discarded because of their low activities. The data set of 75 ligands were segregated into training set of 60 ligands and test set of 15 ligands by considering the fact that test set molecules should represent high, middle and low activities. Molecular modeling studies were performed using the modeling package SYBYL 7.2<sup>21</sup> in a Linux system. The structures of the data set were sketched and minimized using Tripos force field<sup>22</sup> until a gradient convergence of 0.005 kcal/mol was achieved. The chemical structures with experimental and predicted biological activity of both training set (**1–60**) and test set (**61–75**) are listed in Table 1. Their IC<sub>50</sub> values binding to rat CB<sub>1</sub> receptor were converted into the  $-\log$  IC<sub>50</sub> (nM) (pIC<sub>50</sub>) and used as dependent variables for the HQSAR analysis.

In HQSAR, each molecule is divided into a series of unique structural fragments that are counted in the bins of a fixed length array to form a molecular hologram.<sup>23</sup> A number of parameters which are related to hologram generation, such as hologram length, fragment size and fragment distinction, affect the HQSAR model. The hologram length controls the number of bins in the hologram fingerprint with 12 default length from 61 to 401. All of the default hologram lengths are prime number to avoid the fragment collision.<sup>21</sup> Fragment size controls the minimum and maximum length of fragments to be included in the hologram fingerprint with the default as 4 and 7, respectively. Molecular fragment generation utilizes the following fragment distinction: atoms (A), bonds (B), connections (C), hydrogen atoms (H), chirality (Ch), and donor and acceptor (DA). To evaluate the hologram generation, numerous models with the various combinations of the parameters were developed. Table 2 shows the statistical results with different combinations of fragment distinction with the default fragment size (4–7). In each model, atoms and bonds are both included in the fragment distinction parameters. The model 13, which uses atoms, bonds, connections, chirality and donor and acceptor as fragment distinctions, exhibits best statistical results with  $q^2$  of 0.763,  $r^2$  of 0.897, standard estimated error of 0.203, hologram length of 71, and optimal number of components of six. It should be noted that when donor and acceptor flag is enabled, the selection of hydrogen flag cannot make the model better, due to the drastic increase in the number of fragments generated when both of these options are considered. For example, model 4, 6, 10 and 13 are better than

**Table 1**

Chemical structures, experimental and predicted activity of training set and test set

Training set			
Compounds	R	Experimental	Predicted
1		6.80	7.36
2		7.46	7.38
3		7.98	7.57
4		7.82	7.63
5		7.50	7.65
6		8.12	7.92
7		7.98	7.92
8		7.83	7.96
9		8.07	8.01
10		7.88	7.57
11		7.58	7.84

(continued on next page)

Table 1 (continued)

Compounds	R	Experimental	Predicted
12		7.64	7.61
13		7.72	7.68
14		7.96	7.90
15		8.07	8.05
16		7.96	8.02
17		8.06	8.10
18		6.95	6.95
19		7.02	6.77
20		6.25	6.35
21		6.71	6.69
22		7.28	7.40
23		8.18	7.58
24		7.74	7.77
25		7.52	7.69
26		7.84	7.72
27		6.95	7.46
28		7.81	7.44
29		7.81	7.94

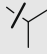
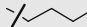
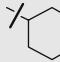
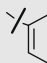
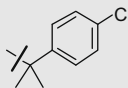
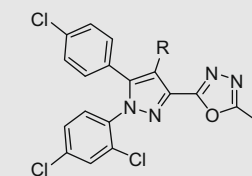
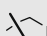
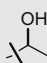
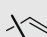
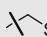
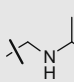
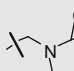
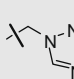
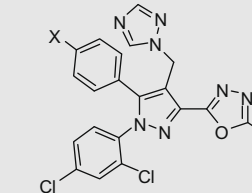
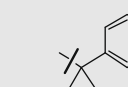
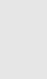
Table 1 (continued)

Compounds	R	Experimental	Predicted
30		7.44	7.65
31		7.44	7.77
32		7.20	7.40
33		7.85	7.87
34		7.31	7.52
35		8.05	8.09
36		7.65	7.65
37		8.32	8.07
38		7.65	7.68
39		8.21	8.04
40		7.54	7.45
41		7.61	7.58
42		7.34	6.96
43		6.64	7.03
44		6.87	7.08
45		7.03	7.14
46		6.54	6.40
47		7.42	7.26

Table 1 (continued)

Compounds	R	Experimental	Predicted
48		7.69	7.74
49		7.73	7.47
50		8.63	8.42
51		7.89	7.86
52		8.47	8.58
X	R	Experimental	Predicted
53	Cl	8.70	8.69
54	Cl	8.82	8.74
55	Cl	8.96	8.99
56	Br <i>t</i> -Bu	8.56	8.74
57	Br	8.55	8.77
58	Br	9.03	9.25
59	Br	8.87	9.06
60	Br	9.24	8.78
Test Set			

Table 1 (continued)

Compounds	R	Experimental	Predicted	
*61		7.60	7.63	
*62		7.14	7.39	
*63		7.92	7.80	
*64		6.55	6.58	
*65		8.32	8.13	
				
*66	<i>n</i> -Pr	7.47	7.81	
*67		7.83	7.80	
*68		8.00	7.58	
*69		7.77	8.02	
*70		7.68	7.93	
*71		7.38	7.16	
*72		6.90	7.11	
*73		8.12	8.34	
				
Compounds	X	R	Experimental	Predicted
*74	Cl		8.66	8.89
*75	Br		9.02	8.83

**Table 2**

Results of HQSAR analyses for various fragment distinction combinations on the key statistical parameters using default fragment size (4–7)

Model	Fragment distinction	$q^2$	$r^2$	SEE	HL	N
1	A/B	0.757	0.892	0.220	307	5
2	A/B/C	0.710	0.862	0.247	401	4
3	A/B/H	0.654	0.894	0.220	307	6
4	A/B/D	0.740	0.851	0.256	97	4
5	A/B/Ch	0.741	0.880	0.232	199	5
6	A/B/C/D	0.731	0.892	0.223	71	6
7	A/B/C/H	0.607	0.879	0.236	257	6
8	A/B/D/H	0.695	0.870	0.244	97	6
9	A/B/C/Ch	0.719	0.887	0.225	257	5
10	A/B/D/Ch	0.747	0.903	0.211	199	6
11	A/B/H/Ch	0.627	0.880	0.234	257	6
12	A/B/C/D/H	0.717	0.903	0.210	151	6
<b>13</b>	<b>A/B/C/D/Ch</b>	<b>0.763</b>	<b>0.897</b>	<b>0.203</b>	<b>71</b>	<b>6</b>
14	A/B/C/H/Ch	0.610	0.887	0.227	257	6
15	A/B/D/H/Ch	0.666	0.870	0.244	97	6
16	A/B/C/D/H/Ch	0.704	0.879	0.235	151	6

The model chosen for analysis is highlighted in bold fonts.

$q^2$ , cross-validated correlation coefficient;  $r^2$ , noncross-validated correlation coefficient; SEE, standard estimated error; HL, hologram length; N, optimal number of components. Fragment distinction: A, atoms; B, bonds; C, connections; H, hydrogen atoms; Ch, chirality; D, donor and acceptor.

**Table 3**

Influence of fragment size on the statistical parameters using the best fragment distinction combinations (atoms, bonds, connections, chirality and donor and acceptor)

Fragment size	$q^2$	$r^2$	SEE	HL	N
2–5	0.728	0.849	0.258	71	4
3–6	0.738	0.892	0.222	83	6
<b>4–7</b>	<b>0.763</b>	<b>0.897</b>	<b>0.203</b>	<b>71</b>	<b>6</b>
5–8	0.738	0.904	0.209	353	6
6–9	0.711	0.911	0.202	307	6
7–10	0.720	0.886	0.226	59	5

The model chosen for analysis is highlighted in bold fonts.

model 8, 12 and 15 and 16, respectively. These results obtained here confirm the previous reports.<sup>18</sup>

The statistical results for the various fragment sizes (including 2–5, 3–6, 4–7, 5–8, 6–9, and 7–10) were evaluated and summarized in Table 3. The table exhibits that further increase or decrease of the fragment size from the default size 4–7 decreased the statistical quality. In HQSAR, the structure encoded within a 2D fingerprint can be directly related to biological activity. Therefore, the HQSAR model generated from training set with 60 compounds was used to predict the biological activity of a test set of structur-

ally related molecules with 15 compounds from its fingerprint. Figure 2 shows the correlation of experimental and predicted activities of both training set and test set from the statistical result of model 13.

The predictive ability of the HQSAR models was expressed with predictive correlation coefficient ( $r^2_{\text{pred}}$ ) defined using Eq. 1:

$$r^2_{\text{pred}} = (\text{SD} - \text{PRESS})/\text{SD} \quad (1)$$

where SD is the sum of squared deviations between the biological activity of the test set and the mean activity of the training set molecules and the PRESS is the sum of squared deviations between predicted and observed activity values for every molecule in the test set.<sup>24</sup> The  $r^2_{\text{pred}}$  for this HQSAR model is 0.868. The high predictive correlation coefficient authenticates the reliability and good predictable capability of the HQSAR model.

HQSAR contribution maps depict the contributions to the biological activities of all the atoms in a molecule structure. Generally, structural units which show poor or intermediate contributions can be identified as potential targets for further modifications.

Figure 3 shows the individual atomic contribution to the activity of most active compounds **20**. The colors at the red end of the spectrum indicate negative contributions, and colors at the green end reflect positive contribution. Atoms with intermediate contributions are colored in white. From Figure 3, it can be seen that the fragments of 1,2,4-triazole ring and cyclopropane ring are strongly related to the biological activity of this compound. Compounds **9**, **50** and **53–60**, which possess 1,2,4-triazole or cyclopropane fragments in the structures of these compounds, all show high biological activities. The nitrogen in 1-position of the pyrazole ring and the oxygen in the 1,3,4-oxadiazole make intermediate-high contributions for the activities. It was reported that in the structural class of 1,5-diaryl-pyrazoles CB1 antagonists, a *para*-substituted phenyl ring at the 5-position of the pyrazole ring and either a 2-chloro or 2,4-dichlorophenyl substitution pattern at 1-position are very important for the CB1 antagonist activity.<sup>25,26</sup> From the present studies of this class of compounds, it was shown that a 1,2,4-triazole structural unit and a cyclopropane moiety at the 5-position of 1,3,4-oxadiazole ring are also important for the biological activities.

The HQSAR contribution map shows that the structural units of 1,3,4-oxadiazoles in the CB-1 antagonists are crucial for the biological activities. In addition, all the antagonists with methyl group on C-4 pyrazole ring show low to mid-low activities (compounds **1–22**), suggesting that modification of the methyl group in this position is necessary. Substitution of methyl with triazolymethyl or tetrazolymethyl group on C-4 pyrazole ring (compounds **50** and **52**) greatly improved binding affinity, which can be explained with the contribution map. Moreover, the 1-phenyl- or 1-trifluoromethylcyclopropyl groups (compounds **54**, **55**, **58**, **59** and **60**) make the antagonists 3–10 times more active than rimonabant. Obviously, the structural units of triazolymethyl or tetrazolymethyl groups and 1-phenyl or 1-trifluoromethyl cyclopropyl groups should be included in new design of CB-1 antagonists based on biarylpyrazolyl oxadiazole scaffold.

In summary, we successfully generated a HQSAR model for biarylpyrazolyl oxadiazole based CB1 antagonists with statistical results in terms of cross-validated  $r^2$  (0.763) and conventional  $r^2$  (0.897). The reliability and the predictable capability of this model were verified by high  $r^2_{\text{pred}}$  value (0.868) using the 15 test set compounds. The contribution maps show that the 1,2,4-triazole or cyclopropane fragments make big contributions for the biological activities. The HQSAR models and the information obtained from the contribution maps might help to design more active CB1 antagonists that are structurally related with the training set compounds.

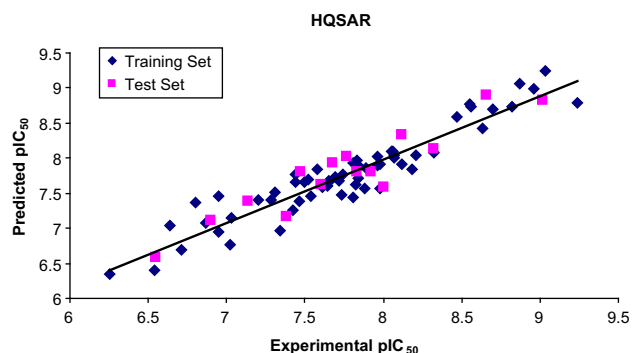


**Figure 2.** Plot of experimental versus predicted  $\text{pIC}_{50}$  values of the training set and test set molecules. The training set and test set molecules are shown in blue (diamond) and pink (squares) spots, respectively.

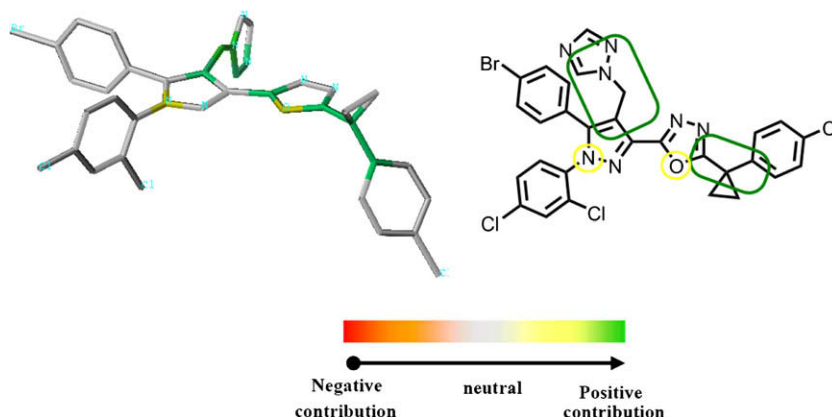


Figure 3. The HQSAR contribution map for most active compound **60**.

## Acknowledgment

The authors gratefully acknowledged the support by U.S. Army Medical Research and Materiel Command Grant (Project No. W81XWH-04-1-0161) for this study.

## References and notes

- Cota, D.; Woods, S. *Curr. Opin. Endocrinol. Diabetes* **2005**, *12*, 338.
- Pagotto, U.; Marsicano, G.; Cota, D.; Lutz, B.; Pasquali, R. *Endocr. Rev.* **2006**, *27*, 73.
- Di Marzo, V.; Bifulco, M.; Petrocellis, L. D. *Nat. Rev. Drug Disc.* **2004**, *3*, 771.
- Petrocellis, L. D.; Cascio, M. G.; Di Marzo, V. *Br. J. Pharmacol.* **2004**, *141*, 765.
- Howlett, A. C.; Breivogel, C. S.; Childers, S. R.; Deadwyler, S. A.; Hampson, R. E.; Porrino, L. J. *Neuropharmacology* **2004**, *47*, 345.
- Boyd, S. T. *Pharmacotherapy* **2006**, *26*, 218.
- Piomelli, D. *Curr. Opin. Invest. Drugs* **2005**, *6*, 672.
- Fride, E.; Ffox, A.; Rosenberg, E.; Faigenboim, M.; Cohen, V. *Eur. J. Pharmacol.* **2003**, *461*, 27.
- Devane, W. A.; Hanus, L.; Breuer, A.; Pertwee, R. G.; Srevenson, L. A.; Griffin, G.; Gibson, D.; Mandelbaum, A.; Etinger, A.; Mechoulam, R. *Science* **1992**, *258*, 1946.
- Devane, W. A.; Dysarz, F. A.; Johnson, M. R.; Melvin, L. S.; Howlett, A. C. *Mol. Pharmacol.* **1988**, *34*, 605.
- Matsuda, L. A.; Lolait, S. J.; Brownstein, M. J.; Young, A. C.; Bonner, T. I. *Nature* **1990**, *346*, 561.
- Lafontan, M.; Piazza, P. V.; Girard, J. *Diabetes Metab.* **2007**, *33*, 85.
- (a) Rinaldi-Carmona, M.; Barth, F.; Héaulme, M.; Alonso, R.; Shire, D.; Congy, C.; Soubrié, P.; Brelière, J.-C.; le Fur, G. *Life Sci.* **1995**, *56*, 1941; (b) Rinaldi-Carmona, M.; Barth, F.; Héaulme, M.; Shire, D.; Calandra, B.; Congy, C.; Martinez, S.; Maruani, J.; Néliat, G.; Caput, D.; Ferrara, P.; Soubrié, P.; Brelière, J.-C.; le Fur, G. *FEBS Lett.* **1994**, *350*, 240.
- (a) Cooke, D.; Bloom, S. *Nat. Rev. Drug Disc.* **2006**, *5*, 919; (b) Lange, J. H. M.; Kruse, C. G. *Drug Discovery Today* **2005**, *10*, 693; (c) Barth, F.; Congy, C.; Martinez, S.; Rinaldi, M. WO97/19063, 2000.; (d) Barth, F.; Casellas, P.; Congy, C.; Martinez, S.; Rinaldi, M. C07D/23114, 1995.; (e) Hutst, D. P.; Lynch, D. L.; Barnett-Norris, J.; Hyatt, S. M.; Seltzman, H. H.; Zhong, M.; Song, Z.-H.; Nie, J.; Lewis, D.; Reggio, P. H. *Mol. Pharmacol.* **2002**, *62*, 1274.
- Lange, J. H. M.; Kruse, C. G. *Drug Discovery Today* **2005**, *10*, 693.
- Lee, S. H.; Seo, H. J.; Lee, S.; Jung, M. E.; Park, J.; Park, H.; Yoo, J.; Yun, H.; Na, J.; Kang, S. Y.; Song, K.; Kim, M.; Chang, C.; Kim, J.; Lee, J. *J. Med. Chem.* **2008**, *51*, 7216.
- Heritage, T. W.; Lowis, D. R. *Molecular Hologram QSAR*. In *Rational Drug Design*; Parrill, A. L., Reddy, M. R., Eds.; ACS Symposium Series 719; American Chemical Society: Washington, DC, 2000; p 212.
- Tripos Sybyl, HQSAR manual.
- (a) Chen, J.; Han, X.; Liu, Q.; Makriyannis, A.; Wang, J.; Xie, X. *J. Med. Chem.* **2006**, *49*, 625; (b) Salo, O. M.; Savinainen, J. R.; Parkkari, T.; Nevalainen, T.; Kakkonen, M. L.; Gynther, J.; Laitinen, J. T.; Järvinen, T.; Poso, A. *J. Med. Chem.* **2006**, *49*, 554; Shim, J. (c) Welsh, W. J.; Cartier, E.; Edwards, J. L.; Howlett, A. C. *J. Med. Chem.* **2002**, *45*, 1447.
- (a) Ye, M.; Dawson, M. I. *Bioorg. Med. Chem. Lett.* **2009**, *19*, 127; (b) Dawson, M. I.; Xia, Z.; Jiang, T.; Ye, M.; Fontana, J. A.; Farhana, L.; Patel, B.; Xue, L.; Bhuiyan, M.; Pellicciari, R.; Macchiariulo, A.; Nuti, R.; Zhang, X.; Han, Y.; Tautz, L.; Hobbs, P. D.; Jong, L.; Waleh, N.; Chao, W.; Feng, G.; Pang, Y.; Su, Y. *J. Med. Chem.* **2008**, *51*, 5650; (c) Dawson, M. I.; Xia, Z.; Liu, G.; Ye, M.; Fontana, J. A.; Farhana, L.; Patel, B.; Arumugarajah, S.; Bhuiyan, M.; Zhang, X.; Han, Y.; Stallcuo, W. B.; Fukushi, J.; Mustelin, T.; Tautz, L.; Su, Y.; Harris, D. L.; Waleh, N.; Hobbs, P. D.; Jong, L.; Chao, W.; Schiff, L. J.; Sani, B. *P. J. Med. Chem.* **2007**, *50*, 2622; (d) Dawson, M. I.; Ye, M.; Cao, X.; Farhana, L.; Hu, Q.; Zhao, Y.; Xu, L.; Kiselyuk, A.; Correa, R. A.; Yang, L.; Hou, T.; Reed, J. C.; Itkin-Ansari, P.; Levine, F.; Sanner, M. F.; Fontana, J. A.; Zhang, X. *ChemMedChem*, **2009**, doi:10.1002/cmdc.200800447.; (e) Ohulchanskyy, T. Y.; Gannon, M. K., II; Ye, M.; Skripchenko, A.; Wagner, S. J.; Prasad, P. N.; Detty, M. R. *J. Phys. Chem. B* **2007**, *111*, 9686; (f) McKnight, R. E.; Ye, M.; Ohulchanskyy, T. Y.; Sahabi, S.; Bryan, R.; Wetzel, B. R.; Wagner, S. J.; Skripchenko, A.; Detty, M. R. *Bioorg. Med. Chem.* **2007**, *15*, 4406; (g) Tomblin, G.; Donnelly, D. J.; Ye, M.; Nygren, C. L.; Detty, M. R. *Biochemistry* **2006**, *45*, 8034; (h) Gibson, S. L.; Holt, J. J.; Ye, M.; Donnelly, D. J.; Ohulchanskyy, T. Y.; You, Y.; Detty, M. R. *Bioorg. Med. Chem.* **2005**, *23*, 6394.
- SYBYL 7.2, Tripos Inc.
- Clark, M.; Cramer, R. D.; Opdenbosch, N. *J. Comput. Chem.* **1989**, *10*, 982.
- (a) Winker, D. A.; Burden, F. R. *Quant. Struct.-Act. Relat.* **1998**, *17*, 224; (b) Seel, M. S.; Turner, D. B.; Willett, P. *Quant. Struct.-Act. Relat.* **1999**, *18*, 245; (c) Tong, W.; Lowis, D. R.; Perkins, R.; Chen, Y.; Welsh, W. J.; Goddette, D. W.; Heritage, T. W.; Sheehan, D. M. *J. Chem. Inf. Comput. Sci.* **1998**, *38*, 669; (d) So, S.-S.; Karplus, M. *J. Comput.-Aided Mol. Des.* **1999**, *13*, 243.
- Cramer, R. D., III; Patterson, D. E.; Bunce, J. D. *J. Am. Chem. Soc.* **1988**, *110*, 5959.
- Lan, R.; Liu, Q.; Fan, P.; Lin, S.; Fernando, S. R. *J. Med. Chem.* **1999**, *42*, 769.
- Francisco, M. E.; Seltzman, H. H.; Gilliam, A. F.; Mitchell, R. A.; Rider, S. L. *J. Med. Chem.* **2002**, *45*, 2708.